Modeling of Spacecraft-Mounted Robot Dynamics and Control Using Dual Quaternions

Alfredo Valverde[1] and Panagiotis Tsiotras[2]

***Abstract*— Dual quaternions (DQ) provide a compact representation of position and attitude. They have been extensively used in fixed-base robotics due to their numerous computational advantages. This paper aims to develop the dynamic equations of motion of a robotic arm on a free-flying spacecraft using a Newton-Euler approach in a DQ modeling framework. A pose-stabilization maneuver for the end-effector is found via Differential Dynamic Programming (DDP). The results of this simulation are provided.**

I. INTRODUCTION

Access to space has enabled a wide range of military and commercial activity. From space-based experimental laboratories, such as the International Space Station (ISS), to missile-tracking defense networks of satellites, to GPS-enabling geostationary satellites that aid our daily commutes, satellites provide valuable services to their operators, the scientific community, and humanity as a whole. Even though launch costs are likely to decrease with the development of reusable first-stage rockets, commercial off-the-shelf (COTS) components, and the miniaturization of components, access to space is, and will remain, expensive for the foreseeable future.

Servicing of orbiting satellites is an essential tool to lower development, equipment and operational costs, as well as to reduce system complexity by means of decreasing required redundancy for a desired lifetime. Satellite servicing encompasses a wide range of uses that aim to extend the satellite lifetime. Common services are visual inspection, scheduled maintenance, refueling, part replacement, repair of worn or broken components, or completion of failed deployment sequences, among others.

A natural approach to satellite servicing is to use robots. However, the operation of a robotic arm on a spacecraft is not a trivial task. Without appropriate dynamical models of the combined system and effective control algorithms, fuel can be quickly depleted, reaction wheels saturated, power drawn too abruptly, a line-of-sight communication link be lost, or the combined system be destabilized. Landmark literature initially proposed the use of active attitude control systems [1], which can be useful in cases when strict pointing requirements exist [2]. However, powerful techniques now exist that allow the base to move freely, or in a reaction-less fashion, during the manipulation of the arm, thus avoiding the aforementioned pitfalls of a free-floating robotic manipulator. Current algorithms have to be able to incorporate changes such as when a payload is released or grabbed, or when there is a significant change in the fuel at the base [3]. Another important component is the incorporation of constraints beyond simple inertial pointing, as in the case of relative attitude constraints between spacecraft to avoid plume impingement, line-of-sight constraints to perform visual navigation, or simple obstacle avoidance constraints to avoid collision between satellites.

The field of multibody dynamics has been thoroughly studied, and it is well-understood. Longman et al. [1] provided a landmark result through conservation of linear momentum. Vafa and Dubowsky [2], [4], [5] introduced the concept of virtual manipulator and the concept of motion of the satellite base through exploitation of the non-holonomicity of the attitude motion relative to joint actuation. Umetami and Yoshida introduced the Generalized Jacobian Matrix (GJM) in [6], and Masutani et al. introduced the use of Lypanuov stability for robotic arms on a free-floating spacecraft in [3]. With this foundation, the study of spacecraft robotics became more formalized, which led to what now we consider robust and efficient algorithms such as those proposed by Jain [7], Rodriguez et al. [8], or Featherstone [9].

Dual quaternions (DQ) have been used in multibody dynamic problems and provide a compact numerical representation of position and attitude (*pose*). They have been applied to obtain fixed-base robotic forward and inverse kinematics, allowing roboticists to reduce computational time and improve precision for common tasks. Several uses of DQ in the literature include the work by Dooley and McCarthy [10], who modeled robotic arm dynamics using the DQ generalized coordinates, Daniilidis [11] and Ulrich [12], who used DQ for hand-eye calibration, Leclercq et al. [13] and Radavelli et al. [14] who demonstrated how to perform kinematic analysis of points, lines and screws using dual quaternions. Dual quaternions have also found use in many other robotics applications such as kinematic analysis of constrained robotic systems [15], [16], singularity avoidance in inverse kinematics [17], and vision-based applications such as SLAM [18], among many others.

Recent work in the field of spacecraft control has focused on the use of dual quaternions to model single rigid body dynamics. The objective of the present paper is to derive the dynamics of a robotic manipulator mounted on a free-floating satellite using dual quaternions and a Newton-Euler approach. Subsequently, the framework is used to command a pose-stabilization maneuver of the end effector.

[1]Alfredo Valverde is a Ph.D. candidate at the School of Aerospace Engineering at the Georgia Institute of Technology, Atlanta, GA 30332-0150, USA, Email: avalverde3@gatech.edu

[2]Panagiotis Tsiotras is the College of Engineering Dean's Professor School of Aerospace Engineering at the Georgia Institute of Technology, Atlanta, GA 30332-0150, USA, Email: tsiotras@gatech.edu

TABLE I
QUATERNION OPERATIONS

Operation	Definition
Addition	$a+b=(a_0+b_0,\bar{a}+\bar{b})$
Mult by scalar	$\lambda a=(\lambda a_0,\lambda a)$
Multiplication	$ab=(a_0b_0-\bar{a}\cdot\bar{b},a_0\bar{b}+b_0\bar{a}+\bar{a}\times\bar{b})$
Conjugate	$a^*=(a_0,-\bar{a})$
Dot product	$a\cdot b=(a_0b_0+\bar{a}\cdot\bar{b},0_{3\times1})$
Cross product	$a\times b=(0,a_0\bar{b}+b_0\bar{a}+\bar{a}\times\bar{b})$
Norm	$\lVert a\rVert=\sqrt{a\cdot a}$

II. MATHEMATICAL PRELIMINARIES

This section introduces the basic concepts of quaternions, dual quaternions, and their use in representing kinematics and dynamics of rigid bodies. For an exhaustive description the reader is referred to [19]–[22], from which the notation has been adopted.

A. Quaternions

The group of quaternions as defined by Hamilton in 1843 extends the well-known imaginary unit j, which satisfies $j^2=-1$. This non-abelian group is defined by the presentation $\mathbb{Q}:=\{-1,i,j,k: i^2=j^2=k^2=ijk=-1\}$. The algebra constructed from $\mathbb{Q}$ over the field of real numbers is the quaternion algebra, $\mathbb{H}$. We can define quaternions as $\mathbb{H}:=\{q=q_0+q_1i+q_2j+q_3k : i^2=j^2=k^2=ijk=-1,\ q_0,q_1,q_2,q_3\in\mathbb{R}\}$. This defines an associative, non-commutative, division algebra.

In practice, quaternions are referred to by their scalar and vectors parts as $q=(q_0,\bar{q})$, where $q_0\in\mathbb{R}$ and $\bar{q}=[q_1,q_2,q_3]^{\mathrm{T}}\in\mathbb{R}^3$. The properties of quaternion algebra are summarized in Table I. Previous literature has defined quaternion multiplication as the multiplication between a 4×4 matrix and a vector in $\mathbb{R}^4$.

Since any rotation can be described by three parameters, the unit norm constraint is imposed on quaternions for attitude representation. *Unit* quaternions are closed under multiplication, but not under addition. A quaternion describing the orientation of frame X with respect to frame Y, $q_{\mathrm{X/Y}}$, will satisfy $q^*_{\mathrm{X/Y}}q_{\mathrm{X/Y}}=q_{\mathrm{X/Y}}q^*_{\mathrm{X/Y}}=1$, where $1=(1,0_{3\times1})$. This quaternion can be constructed as $q_{\mathrm{X/Y}}=(\cos(\phi/2),\bar{n}\sin(\theta/2))$, where $\bar{n}$ and θ are the *unit* Euler axis, and Euler angle of the rotation respectively. It is worth emphasizing that $q^*_{\mathrm{Y/X}}=q_{\mathrm{X/Y}}$, and that $q_{\mathrm{X/Y}}$ and $-q_{\mathrm{X/Y}}$ represent the same rotation. Furthermore, given quaternions $q_{\mathrm{Y/X}}$ and $q_{\mathrm{Z/Y}}$, the quaternion describing the rotation from X to Z is given by $q_{\mathrm{Z/X}}=q_{\mathrm{Y/X}}q_{\mathrm{Z/Y}}$.

Three-dimensional vectors can be interpreted as quaternions. For example, given $\bar{s}^{\mathrm{X}}\in\mathbb{R}^3$, the coordinates of a vector expressed in frame X, its quaternion representation is given by $s^{\mathrm{X}}=(0,\bar{s}^{\mathrm{X}})\in\mathbb{H}^v$, where $\mathbb{H}^v$ is the set of *vector* quaternions defined as $\mathbb{H}^v\triangleq\{(q_0,\bar{q})\in\mathbb{H}:\ q_0=0\}$ (see [21] for further information). The change of reference frame on a vector quaternion is achieved by the adjoint operation, and is given by $s^{\mathrm{Y}}=q^*_{\mathrm{Y/X}}s^{\mathrm{X}}q_{\mathrm{Y/X}}$. Additionally, given $s\in\mathbb{H}^v$, we can define the operation $[\cdot]^\times:\mathbb{H}^v\to\mathbb{R}^{4\times4}$ as

$$[s]^\times=\begin{bmatrix}0 & 0_{1\times3}\\ 0_{3\times1} & [\bar{s}]^\times\end{bmatrix}, \tag{1}$$

where $[\bar{s}]^\times$ is the skew-symmetric matrix such that $[\bar{s}]^\times\bar{a}=\bar{s}\times\bar{a}$.

In general, the attitude kinematics evolve as

$$\dot{q}_{\mathrm{X/Y}}=\tfrac{1}{2}q_{\mathrm{X/Y}}\omega^{\mathrm{X}}_{\mathrm{X/Y}}=\tfrac{1}{2}\omega^{\mathrm{Y}}_{\mathrm{X/Y}}q_{\mathrm{X/Y}}, \tag{2}$$

where $\omega^{\mathrm{Z}}_{\mathrm{X/Y}}\triangleq(0,\bar{\omega}^{\mathrm{Z}}_{\mathrm{X/Y}})\in\mathbb{H}^v$ and $\bar{\omega}^{\mathrm{Z}}_{\mathrm{X/Y}}\in\mathbb{R}^3$ is the angular velocity of frame X with respect to frame Y expressed in Z-frame coordinates.

B. Dual Quaternions

Dual quaternion algebra is defined as $\mathbb{H}_d=\{\boldsymbol{q}=q_r+\epsilon q_d : q_r,q_d\in\mathbb{H}\}$, and ϵ is the dual unit. We call q_r the real part, and q_d the dual part.

Filipe et al. [19]–[22] have laid out much of the groundwork in terms of the notation and the basic properties of dual quaternions. The main properties of dual quaternion algebra are listed in Table II. Reference [23] also conveniently defines a multiplication between matrices and dual quaternions that resembles the well-known matrix-vector multiplication by simply representing the dual quaternion coefficients as a vector in $\mathbb{R}^8$. A property that arises from the definition of the circle product for dual quaternions is given as follows

TABLE II
DUAL QUATERNION OPERATIONS

Operation	Definition
Addition	$\boldsymbol{a}+\boldsymbol{b}=(a_r+b_r)+\epsilon(a_d+b_d)$
Mult by scalar	$\lambda\boldsymbol{a}=(\lambda a_r)+\epsilon(\lambda a_d)$
Multiplication	$\boldsymbol{ab}=(a_rb_r)+\epsilon(a_db_r+a_rb_d)$
Conjugate	$\boldsymbol{a}^*=(a_r^*)+\epsilon(a_d^*)$
Dot product	$\boldsymbol{a}\cdot\boldsymbol{b}=(a_r\cdot b_r)+\epsilon(a_d\cdot b_r+a_r\cdot b_d)$
Cross product	$\boldsymbol{a}\times\boldsymbol{b}=(a_r\times b_r)+\epsilon(a_d\times b_r+a_r\times b_d)$
Circle product	$\boldsymbol{a}\circ\boldsymbol{b}=(a_r\cdot b_r+a_d\cdot b_d)+\epsilon 0$
Swap	$\boldsymbol{a}^{\mathrm{s}}=a_d+\epsilon a_r$
Norm	$\lVert a\rVert=\sqrt{a\circ a}$
Vector part	$\mathrm{vec}(\boldsymbol{a})=(0,\overline{a_r})+\epsilon(0,\overline{a_d})$

$$\boldsymbol{a}^{\mathrm{s}}\circ\boldsymbol{b}^{\mathrm{s}}=\boldsymbol{a}\circ\boldsymbol{b}=\boldsymbol{b}\circ\boldsymbol{a}. \tag{3}$$

Analogous to the set of vector quaternions $\mathbb{H}^v$, we can define the set of vector dual quaternions as $\mathbb{H}^v_d\triangleq\{\boldsymbol{q}=q_r+\epsilon q_d :\ q_r,q_d\in\mathbb{H}^v\}$. Vector dual quaternions have special properties of interest in the study of kinematics, dynamics and control of rigid bodies. The two main properties are listed below, where $\boldsymbol{a},\boldsymbol{b}\in\mathbb{H}^v_d$:

$$\boldsymbol{a}\circ(\boldsymbol{bc})=\boldsymbol{b}^{\mathrm{s}}\circ(\boldsymbol{a}^{\mathrm{s}}\boldsymbol{c}^*)=\boldsymbol{c}^{\mathrm{s}}\circ(\boldsymbol{b}^*\boldsymbol{a}^{\mathrm{s}}), \tag{4}$$

$$\boldsymbol{a}\circ(\boldsymbol{b}\times\boldsymbol{c})=\boldsymbol{b}^{\mathrm{s}}\circ(\boldsymbol{c}\times\boldsymbol{a}^{\mathrm{s}})=\boldsymbol{c}^{\mathrm{s}}\circ(\boldsymbol{a}^{\mathrm{s}}\times\boldsymbol{b}). \tag{5}$$

Finally, for vector dual quaternions we will define the skew-symmetric operator $[\cdot]^\times:\mathbb{H}^v_d\to\mathbb{R}^{8\times8}$,

$$[\boldsymbol{s}]^\times=\begin{bmatrix}[s_r]^\times & 0_{4\times4}\\ [s_d]^\times & [s_r]^\times\end{bmatrix}. \tag{6}$$

Since rigid body motion has six degrees of freedom, a dual quaternion needs two constraints to parameterize it. The dual quaternion describing the relative pose of frame B relative to I is given by $\boldsymbol{q}_{\mathrm{B/I}} = q_{\mathrm{B/I},r} + \epsilon q_{\mathrm{B/I},d} = q_{\mathrm{B/I}} + \epsilon \frac{1}{2} q_{\mathrm{B/I}} r^{\mathrm{B}}_{\mathrm{B/I}}$, where $r^{\mathrm{B}}_{\mathrm{B/I}}$ is the position quaternion describing the location of the origin of frame B relative to that of frame I, expressed in B-frame coordinates. It can be easily observed that $q_{\mathrm{B/I},r} \cdot q_{\mathrm{B/I},r} = \mathtt{1}$ and $q_{\mathrm{B/I},r} \cdot q_{\mathrm{B/I},d} = \mathtt{0}$, where $\mathtt{0} = (0, \bar{0})$, providing the two necessary constraints. Thus, a dual quaternion representing a pose transformation is actually a *unit* dual quaternion, since it satisfies $\boldsymbol{q} \cdot \boldsymbol{q} = \boldsymbol{q}^* \boldsymbol{q} = \mathbf{1}$, where $\mathbf{1} = \mathtt{1} + \epsilon \mathtt{0}$. We will also define $\mathbf{0} = \mathtt{0} + \epsilon \mathtt{0}$.

Frame transformations can be performed with the adjoint operation on a dual vector as $\boldsymbol{s}^{\mathrm{Y}} = \boldsymbol{q}^*_{\mathrm{Y/X}} \boldsymbol{s}^{\mathrm{X}} \boldsymbol{q}_{\mathrm{Y/X}}$ for $\boldsymbol{s}^{\mathrm{Y}}, \boldsymbol{s}^{\mathrm{X}} \in \mathbb{H}^v_d$. Also, similar to quaternion relationships, dual quaternions satisfy the following properties: $\boldsymbol{q}_{\mathrm{Z/X}} = \boldsymbol{q}_{\mathrm{Y/X}} \boldsymbol{q}_{\mathrm{Z/Y}}$ and $\boldsymbol{q}^*_{\mathrm{Y/X}} = \boldsymbol{q}_{\mathrm{X/Y}}$.

The dual velocity is defined as

$$\boldsymbol{\omega}^{\mathrm{X}}_{\mathrm{Y/Z}} = \boldsymbol{q}^*_{\mathrm{X/Y}} \boldsymbol{\omega}^{\mathrm{Y}}_{\mathrm{Y/Z}} \boldsymbol{q}_{\mathrm{X/Y}} = \omega^{\mathrm{X}}_{\mathrm{Y/Z}} + \epsilon (v^{\mathrm{X}}_{\mathrm{Y/Z}} + \omega^{\mathrm{X}}_{\mathrm{Y/Z}} \times r^{\mathrm{X}}_{\mathrm{X/Y}}). \tag{7}$$

and contains both the linear and and the angular velocities of the body. The dual velocity of a rigid body, assigned to frame B, with respect to the inertial frame is defined as $\boldsymbol{\omega}^{\mathrm{B}}_{\mathrm{B/I}} = \omega^{\mathrm{B}}_{\mathrm{B/I}} + \epsilon v^{\mathrm{B}}_{\mathrm{B/I}}$. The dual quaternion kinematics can be expressed as

$$\dot{\boldsymbol{q}}_{\mathrm{X/Y}} = \tfrac{1}{2} \boldsymbol{q}_{\mathrm{X/Y}} \boldsymbol{\omega}^{\mathrm{X}}_{\mathrm{X/Y}} = \tfrac{1}{2} \boldsymbol{\omega}^{\mathrm{Y}}_{\mathrm{X/Y}} \boldsymbol{q}_{\mathrm{X/Y}}. \tag{8}$$

C. Dynamics in Dual Quaternion Algebra

In [23], the authors represent the 6-DOF dynamics of a rigid body i by

$$M_{\odot_{\mathrm{i}}} \star (\dot{\boldsymbol{\omega}}^{\odot_{\mathrm{i}}}_{\odot_{\mathrm{i}}/\mathrm{I}})^{\mathrm{s}} + \boldsymbol{\omega}^{\odot_{\mathrm{i}}}_{\odot_{\mathrm{i}}/\mathrm{I}} \times \left(M_{\odot_{\mathrm{i}}} \star (\boldsymbol{\omega}^{\odot_{\mathrm{i}}}_{\odot_{\mathrm{i}}/\mathrm{I}})^{\mathrm{s}}\right) = \boldsymbol{W}^{\odot_{\mathrm{i}}}_{\mathrm{i}}(O_{\odot_{\mathrm{i}}}), \tag{9}$$

where $\boldsymbol{W}^{\odot_{\mathrm{i}}}_{\mathrm{i}}(O_{\odot_{\mathrm{i}}}) = f^{\odot_{\mathrm{i}}} + \epsilon \tau^{\odot_{\mathrm{i}}}$ is the wrench expressed in the $\odot_{\mathrm{i}}$ frame, whose origin is at the center of mass, computed about the center of mass, and I is the inertial reference frame. The matrix $M_{\odot_{\mathrm{i}}} \in \mathbb{R}^{8\times 8}$ is the *dual inertia matrix* defined as

$$M_{\odot_{\mathrm{i}}} = \begin{bmatrix} 1 & 0_{1\times 3} & 0 & 0_{1\times 3} \\ 0_{3\times 1} & m_{\mathrm{i}} I_{3\times 3} & 0_{3\times 1} & 0_{3\times 3} \\ 0 & 0_{1\times 3} & 1 & 0_{1\times 3} \\ 0_{3\times 1} & 0_{3\times 3} & 0_{3\times 1} & \bar{I}_{\odot_{\mathrm{i}}} \end{bmatrix}, \tag{10}$$

where $\bar{I}_{\odot_{\mathrm{i}}} \in \mathbb{R}^{3\times 3}$ is the mass moment of inertia of the body about the center of mass, and m_{i} is the mass of the body. Finally, we define the following operators: $[\![\,\cdot\,]\!]_{\mathrm{L}}, [\![\,\cdot\,]\!]_{\mathrm{R}} : \mathbb{H}_d \to \mathbb{R}^{8\times 8}$ such that $\boldsymbol{a}\boldsymbol{b} \triangleq [\![\boldsymbol{a}]\!]_{\mathrm{L}} \star b \triangleq [\![\boldsymbol{b}]\!]_{\mathrm{R}} \star \boldsymbol{a}$, and $\mathrm{H}(\cdot) : \mathbb{R}^{8\times 8} \to \mathbb{R}^{8\times 8}$ such that $\mathrm{H}(M) \star \boldsymbol{a} \triangleq M \star \boldsymbol{a}^{\mathrm{s}}$.

III. DYNAMICS OF A ROBOTIC ARM ON A SPACECRAFT

The dynamics will be derived using dual quaternion algebra for the satellite with an RRRS (R - revolute, S - spherical) joint configuration shown in Figure 1. The diagram shows reference frames, reaction forces and torques, actuation torques, points of interest (all with attached reference frames), and external forces and torques applied at the centers of mass and at the end effector. The joint degrees of freedom have not been labeled. The R joints add a degree of freedom along the Z-axis of the local frame (of the distal body). These are, respectively, parameterized by the angles $\theta_{1/0}$, $\theta_{2/1}$, and $\theta_{3/2}$. The motion of the S joint is described by a 3-2-1 Euler angle rotation parameterized by $\psi_{\mathrm{e}/\odot_3}$, $\theta_{\mathrm{e}/\odot_3}$, $\phi_{\mathrm{e}/\odot_3}$. The state of the system

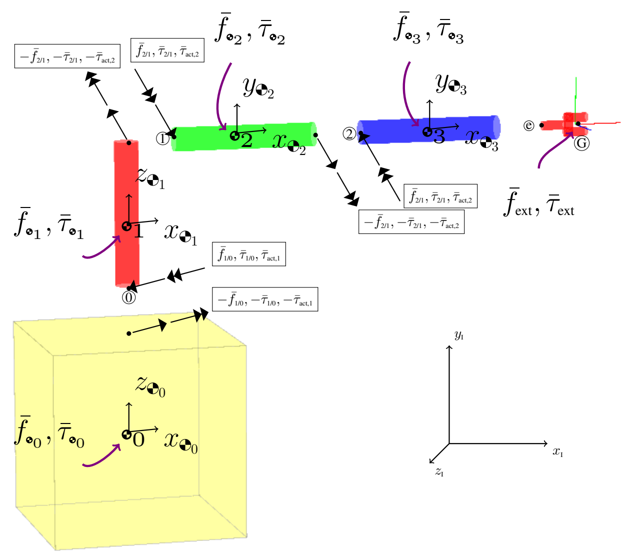

Fig. 1. Exploded satellite view.

is described by $\boldsymbol{x} = [\boldsymbol{q}^{\mathrm{T}}_{\odot_0/\mathrm{I}}, \theta_{1/0}, \theta_{2/1}, \theta_{3/2}, \psi_{\mathrm{e}/\odot_3}, \theta_{\mathrm{e}/\odot_3}, \phi_{\mathrm{e}/\odot_3}, \boldsymbol{y}^{\mathrm{T}}]^{\mathrm{T}} \in \mathbb{R}^{46}$, where $\boldsymbol{y} = [\boldsymbol{\omega}^{\odot_0\,\mathrm{T}}_{\odot_0/\mathrm{I}}, \boldsymbol{\omega}^{\odot_1\,\mathrm{T}}_{\odot_1/\mathrm{I}}, \boldsymbol{\omega}^{\odot_2\,\mathrm{T}}_{\odot_2/\mathrm{I}}, \boldsymbol{\omega}^{\odot_3\,\mathrm{T}}_{\odot_3/\mathrm{I}}]^{\mathrm{T}} \in \mathbb{R}^{32}$. The control inputs are taken to be $\boldsymbol{u}(t) = [\boldsymbol{W}^{\odot_0}_{\odot_0}(O_{\odot_0})^{\mathrm{T}}, (\bar{\tau}_{\mathrm{act},1})_z, (\bar{\tau}_{\mathrm{act},2})_z, (\bar{\tau}_{\mathrm{act},3})_z, \dot{\psi}_{\mathrm{e}/\odot_3}, \dot{\theta}_{\mathrm{e}/\odot_3}, \dot{\phi}_{\mathrm{e}/\odot_3}]^{\mathrm{T}} \in \mathbb{R}^{14}$. From Equation (8), the pose of the base evolves as

$$\dot{\boldsymbol{q}}_{\odot_0/\mathrm{I}} = \tfrac{1}{2} \boldsymbol{q}_{\odot_0/\mathrm{I}} \boldsymbol{\omega}^{\odot_0}_{\odot_0/\mathrm{I}}. \tag{11}$$

We can extract revolute joint angular velocities as

$$\begin{aligned} \dot{\theta}_{\mathrm{i+1/i}} &= [0,0,0,1,0,0,0,0]\boldsymbol{\omega}^{\mathrm{i}}_{\mathrm{i}/\odot_{\mathrm{i}}} \\ &= [0,0,0,1,0,0,0,0]\left(\boldsymbol{q}_{\odot_{\mathrm{i}+1}/\mathrm{i}} \boldsymbol{\omega}^{\odot_{\mathrm{i}+1}}_{\odot_{\mathrm{i}+1}/\mathrm{I}} \boldsymbol{q}^*_{\odot_{\mathrm{i}+1}/\mathrm{i}} - \boldsymbol{q}^*_{\mathrm{i}/\odot_{\mathrm{i}}} \boldsymbol{\omega}^{\odot_{\mathrm{i}}}_{\odot_{\mathrm{i}}/\mathrm{I}} \boldsymbol{q}_{\mathrm{i}/\odot_{\mathrm{i}}}\right). \end{aligned} \tag{12}$$

Assuming that the end-effector is massless, solely affecting the kinematics, we need only to derive expressions for $\dot{\boldsymbol{y}}$. Computing Equation (9) for each of the four bodies, eliminating the swap operator, moving unknowns to the left-hand side, and transporting the applied wrenches to the center of mass of each body, we get

$$\begin{aligned} &\mathrm{H}(M_{\odot_0}) \star \dot{\boldsymbol{\omega}}^{\odot_0}_{\odot_0/\mathrm{I}} + [\![\boldsymbol{q}_{0/\odot_0}]\!]_{\mathrm{L}} [\![\boldsymbol{q}^*_{0/\odot_0}]\!]_{\mathrm{R}} \boldsymbol{E}^{\mathrm{T}}_{158} \tilde{\boldsymbol{W}}^{\odot_1}_{1/0}(O_0) \\ &= -\boldsymbol{\omega}^{\odot_0}_{\odot_0/\mathrm{I}} \times \left(M_{\odot_0} \star (\boldsymbol{\omega}^{\odot_0}_{\odot_0/\mathrm{I}})^{\mathrm{s}}\right) + \boldsymbol{W}^{\odot_0}_{\odot_0}(O_{\odot_0}) - \boldsymbol{q}_{0/\odot_0} \boldsymbol{W}^{\odot_1}_{\mathrm{act},1}(O_0) \boldsymbol{q}^*_{0/\odot_0}, \end{aligned} \tag{13}$$

$$\begin{aligned} &\mathrm{H}(M_{\odot_1}) \star \dot{\boldsymbol{\omega}}^{\odot_1}_{\odot_1/\mathrm{I}} - [\![\boldsymbol{q}^*_{\odot_1/0}]\!]_{\mathrm{L}} [\![\boldsymbol{q}_{\odot_1/0}]\!]_{\mathrm{R}} \boldsymbol{E}^{\mathrm{T}}_{158} \tilde{\boldsymbol{W}}^{\odot_1}_{1/0}(O_0) \\ &+ [\![\boldsymbol{q}_{1/\odot_1}]\!]_{\mathrm{L}} [\![\boldsymbol{q}^*_{1/\odot_1}]\!]_{\mathrm{R}} \boldsymbol{E}^{\mathrm{T}}_{158} \tilde{\boldsymbol{W}}^{\odot_2}_{2/1}(O_1) = -\boldsymbol{\omega}^{\odot_1}_{\odot_1/\mathrm{I}} \times \left(M_{\odot_1} \star (\boldsymbol{\omega}^{\odot_1}_{\odot_1/\mathrm{I}})^{\mathrm{s}}\right) \\ &+ \boldsymbol{W}^{\odot_1}_{\odot_1}(O_{\odot_1}) + \boldsymbol{q}^*_{\odot_1/0} \boldsymbol{W}^{\odot_1}_{\mathrm{act},1}(O_0) \boldsymbol{q}_{\odot_1/0} - \boldsymbol{q}_{1/\odot_1} \boldsymbol{W}^{\odot_2}_{\mathrm{act},2}(O_1) \boldsymbol{q}^*_{1/\odot_1}, \end{aligned} \tag{14}$$

$$\begin{aligned} &\mathrm{H}(M_{\odot_2}) \star \dot{\boldsymbol{\omega}}^{\odot_2}_{\odot_2/\mathrm{I}} - [\![\boldsymbol{q}^*_{\odot_2/1}]\!]_{\mathrm{L}} [\![\boldsymbol{q}_{\odot_2/1}]\!]_{\mathrm{R}} \boldsymbol{E}^{\mathrm{T}}_{158} \tilde{\boldsymbol{W}}^{\odot_2}_{2/1}(O_1) \\ &+ [\![\boldsymbol{q}_{2/\odot_2}]\!]_{\mathrm{L}} [\![\boldsymbol{q}^*_{2/\odot_2}]\!]_{\mathrm{R}} \boldsymbol{E}^{\mathrm{T}}_{158} \tilde{\boldsymbol{W}}^{\odot_3}_{3/2}(O_2) = -\boldsymbol{\omega}^{\odot_2}_{\odot_2/\mathrm{I}} \times \left(M_{\odot_2} \star (\boldsymbol{\omega}^{\odot_2}_{\odot_2/\mathrm{I}})^{\mathrm{s}}\right) \\ &+ \boldsymbol{W}^{\odot_2}_{\odot_2}(O_{\odot_2}) + \boldsymbol{q}^*_{\odot_2/1} \boldsymbol{W}^{\odot_2}_{\mathrm{act},2}(O_1) \boldsymbol{q}_{\odot_2/1} - \boldsymbol{q}_{2/\odot_2} \boldsymbol{W}^{\odot_3}_{\mathrm{act},3}(O_2) \boldsymbol{q}^*_{2/\odot_2}, \end{aligned} \tag{15}$$

$$
\begin{aligned}
&\mathrm{H}\left(M_{\odot_3}\right) \star \dot{\boldsymbol{\omega}}^{\odot_3}_{\odot_3/\mathrm{I}} - \left[\!\left[\boldsymbol{q}^*_{\odot_3/2} \right]\!\right]_{\mathrm{L}} \left[\!\left[\boldsymbol{q}_{\odot_3/2} \right]\!\right]_{\mathrm{R}} \boldsymbol{E}^{\mathrm{T}}_{158} \tilde{\boldsymbol{W}}^{\odot_3}_{3/2}(O_2) \\
&= -\boldsymbol{\omega}^{\odot_3}_{\odot_3/\mathrm{I}} \times \left(M_{\odot_3} \star (\boldsymbol{\omega}^{\odot_3}_{\odot_3/\mathrm{I}})^{\mathsf{s}}\right) + \boldsymbol{W}^{\odot_3}_{\odot_3}(O_{\odot_3}) \\
&\quad + \boldsymbol{q}^*_{\odot_3/2} \boldsymbol{W}^{\odot_3}_{\mathrm{act},3}(O_2) \boldsymbol{q}_{\odot_3/2} + \boldsymbol{q}_{\mathrm{G}/\odot_3} \boldsymbol{W}^{G}_{\mathrm{ext}}(O_G) \boldsymbol{q}^*_{\mathrm{G}/\odot_3}.
\end{aligned} \tag{16}
$$

Here, we have defined $E_{158} \in \mathbb{R}^{5\times 8}$ to be the eight-dimensional identity matrix without rows one, five and eight, allowing us to remove non-zero entries of the reaction wrenches, which we have denoted as $\tilde{\boldsymbol{W}}$.

Finally, we need only to express the velocity constraints in a similar fashion for each of the joints. The dual velocity of the joints can be related via

$$
\boldsymbol{\omega}^{\odot_{i+1}}_{\odot_{i+1}/\mathrm{I}} = \boldsymbol{\omega}^{\odot_{i+1}}_{\odot_{i+1}/\mathrm{i}} + \boldsymbol{\omega}^{\odot_{i+1}}_{\mathrm{i}/\odot_i} + \boldsymbol{\omega}^{\odot_{i+1}}_{\odot_i/\mathrm{I}}, \tag{17}
$$

Taking a time derivative and clearing of transformations the dual acceleration of the joint in the local frame, the constraint for joint i is given by

$$
\boldsymbol{q}_{\odot_{i+1}/\mathrm{i}} \dot{\boldsymbol{\omega}}^{\odot_{i+1}}_{\odot_{i+1}/\mathrm{I}} \boldsymbol{q}^*_{\odot_{i+1}/\mathrm{i}} = \dot{\boldsymbol{\omega}}^{\mathrm{i}}_{\mathrm{i}/\odot_i} + \boldsymbol{q}^*_{\mathrm{i}/\odot_i} \left(\dot{\boldsymbol{\omega}}^{\odot_i}_{\odot_i/\mathrm{I}} + \boldsymbol{\omega}^{\odot_i}_{\odot_i/\mathrm{I}} \times \boldsymbol{\omega}^{\odot_i}_{\mathrm{i}/\odot_i} \right) \boldsymbol{q}_{\mathrm{i}/\odot_i}. \tag{18}
$$

Multiplying this equation by E_{145}, defined similarly to E_{158}, on the left, will cancel the joint acceleration, which was redundant given that we are solving for angular acceleration of the bodies. This yields the i-th joint constraint:

$$
\begin{aligned}
&\boldsymbol{E}_{145} \left[\!\left[\boldsymbol{q}_{\odot_{i+1}/\mathrm{i}} \right]\!\right]_{\mathrm{L}} \left[\!\left[\boldsymbol{q}^*_{\odot_{i+1}/\mathrm{i}} \right]\!\right]_{\mathrm{R}} \star \dot{\boldsymbol{\omega}}^{\odot_{i+1}}_{\odot_{i+1}/\mathrm{I}} - \boldsymbol{E}_{145} \left[\!\left[\boldsymbol{q}^*_{\mathrm{i}/\odot_i} \right]\!\right]_{\mathrm{L}} \left[\!\left[\boldsymbol{q}_{\mathrm{i}/\odot_i} \right]\!\right]_{\mathrm{R}} \star \dot{\boldsymbol{\omega}}^{\odot_i}_{\odot_i/\mathrm{I}} \\
&= \boldsymbol{E}_{145} \boldsymbol{q}^*_{\mathrm{i}/\odot_i} \left(\boldsymbol{\omega}^{\odot_i}_{\odot_i/\mathrm{I}} \times \boldsymbol{\omega}^{\odot_i}_{\mathrm{i}/\odot_i} \right) \boldsymbol{q}_{\mathrm{i}/\odot_i}.
\end{aligned} \tag{19}
$$

Defining $\boldsymbol{\mathcal{T}} \triangleq [\tilde{\boldsymbol{W}}^{\odot_1}_{1/0}(O_0)^{\mathrm{T}}, \tilde{\boldsymbol{W}}^{\odot_2}_{2/1}(O_1)^{\mathrm{T}}, \tilde{\boldsymbol{W}}^{\odot_3}_{3/2}(O_2)^{\mathrm{T}}]^{\mathrm{T}}$, we can cast Equations (13) to (16) and Equation (19) for i $\in \{0, 1, 2\}$ in the form of a linear system of equations given by

$$
\begin{bmatrix} \boldsymbol{\mathcal{S}}_{11} & \boldsymbol{\mathcal{S}}_{12} \\ \boldsymbol{\mathcal{S}}_{21} & \boldsymbol{\mathcal{S}}_{22} \end{bmatrix} \begin{bmatrix} \dot{\boldsymbol{y}} \\ \boldsymbol{\mathcal{T}} \end{bmatrix} = \begin{bmatrix} \boldsymbol{\mathcal{B}}_1 \\ \boldsymbol{\mathcal{B}}_2 \end{bmatrix}. \tag{20}
$$

Using the fact that $\boldsymbol{\mathcal{S}}_{22} = 0_{15\times 15}$, we can solve (20) to obtain

$$
\boldsymbol{\mathcal{T}} = (\boldsymbol{\mathcal{S}}_{21}\boldsymbol{\mathcal{S}}_{11}^{-1}\boldsymbol{\mathcal{S}}_{12})^{-1}(\boldsymbol{\mathcal{S}}_{21}\boldsymbol{\mathcal{S}}_{11}^{-1}\boldsymbol{\mathcal{B}}_1 - \boldsymbol{\mathcal{B}}_2), \tag{21}
$$

$$
\dot{\boldsymbol{y}} = -\boldsymbol{\mathcal{S}}_{11}^{-1}\boldsymbol{\mathcal{S}}_{12}\boldsymbol{\mathcal{T}} + \boldsymbol{\mathcal{S}}_{11}^{-1}\boldsymbol{\mathcal{B}}_1. \tag{22}
$$

These formulas provide the dual accelerations $\dot{\boldsymbol{y}}$ and constraint wrenches $\boldsymbol{\mathcal{T}}$ as a function of the satellite configuration and the applied external and actuation wrenches.

IV. END EFFECTOR CONTROL USING DDP

To solve the problem of stabilizing the end-effector at a given desired pose, we use Differential Dynamic Programming (DDP). DDP aims to minimize the cost functional

$$
J(x_0, U) = \mathcal{L}_f(x_N, N) + \sum_{k=0}^{N-1} \mathcal{L}(x_k, u_k, k) \tag{23}
$$

with respect to $U = \{u_k\}_{k=0}^{k=N-1}$. To do this, DDP performs a forward-backward propagation of the state and the value function, respectively, based on the Bellman principle, which in discrete time is given by

$$
V(x_k, k) = \min_{u_k} Q(x_k, u_k, k). \tag{24}
$$

Here $Q(x_k, u_k, k)$ is an auxiliary function that includes the running cost and the cost-to-go and it is defined as

$$
Q(x_k, u_k, k) \triangleq \mathcal{L}(x_k, u_k, k) + V(x_{k+1}, k+1). \tag{25}
$$

The specific implementation used for control in this section is based on the work described in [24]. One of the innovations in [24] is the ability to incorporate control limits (i.e., saturation limits) during planning, avoiding the negative consequences of simply clipping control inputs during implementation. Additionally, the authors of [24] make use of a backtracking search parameter, $\alpha \in \mathbb{R}$, to perform a line search on the optimal update of the control input. That way, for a given iteration of DDP, a sweep of control policies is parameterized by $\alpha \in [0, 1]$ as follows

$$
\delta u^*(t_k; \alpha) = -Q_{uu}^{-1} Q_{ux} \delta x(t_k) - \alpha Q_{uu}^{-1} Q_u^{\mathrm{T}}, \tag{26}
$$

and then one selects the update with the best performance, where in (**??**) the subscripts in Q denote partial derivatives.

In order to aid the convergence of the algorithm, the pose of the end effector with respect to the inertial frame $\boldsymbol{q}_{\mathrm{G/I}}$ was added as a state to the formulation. This implies the need to derive the kinematics of the end effector. In dual quaternion algebra this is a simple derivation which we provide below.

Consider the pose of the end effector as the chain of relative pose transformations given by

$$
\boldsymbol{q}_{\mathrm{G/I}} = \boldsymbol{q}_{\odot_0/\mathrm{I}} \boldsymbol{q}_{0/\odot_0} \boldsymbol{q}_{\odot_1/0} \boldsymbol{q}_{1/\odot_1} \boldsymbol{q}_{\odot_2/1} \boldsymbol{q}_{2/\odot_2} \boldsymbol{q}_{\odot_3/2} \boldsymbol{q}_{\mathrm{e}/\odot_3} \boldsymbol{q}_{\mathrm{G/e}}. \tag{27}
$$

The dual quaternions $\boldsymbol{q}_{\odot_1/0}, \boldsymbol{q}_{\odot_2/1}, \boldsymbol{q}_{\odot_3/2}, \boldsymbol{q}_{\mathrm{G/e}}$ are constant, and their derivatives are **0** because they represent pose transformations along the same rigid body. Therefore, using Equation (8) we can easily take the derivative of $\boldsymbol{q}_{\mathrm{G/I}}$ as

$$
\begin{aligned}
\dot{\boldsymbol{q}}_{\mathrm{G/I}} &= \dot{\boldsymbol{q}}_{\odot_0/\mathrm{I}} \boldsymbol{q}_{\mathrm{G}/\odot_0} + \boldsymbol{q}_{\odot_0/\mathrm{I}} \dot{\boldsymbol{q}}_{0/\odot_0} \boldsymbol{q}_{\mathrm{G}/0} + \boldsymbol{q}_{\odot_1/\mathrm{I}} \dot{\boldsymbol{q}}_{1/\odot_1} \boldsymbol{q}_{\mathrm{G}/1} \\
&\quad + \boldsymbol{q}_{\odot_2/\mathrm{I}} \dot{\boldsymbol{q}}_{2/\odot_2} \boldsymbol{q}_{\mathrm{G}/2} + \boldsymbol{q}_{\odot_3/\mathrm{I}} \dot{\boldsymbol{q}}_{\mathrm{e}/\odot_3} \boldsymbol{q}_{\mathrm{G/e}}
\end{aligned} \tag{28}
$$

$$
\begin{aligned}
\dot{\boldsymbol{q}}_{\mathrm{G/I}} &= \tfrac{1}{2} \boldsymbol{q}_{\odot_0/\mathrm{I}} \boldsymbol{\omega}^{\odot_0}_{\odot_0/\mathrm{I}} \boldsymbol{q}_{\mathrm{G}/\odot_0} + \tfrac{1}{2} \boldsymbol{q}_{\odot_0/\mathrm{I}} \boldsymbol{\omega}^{\odot_0}_{0/\odot_0} \boldsymbol{q}_{0/\odot_0} \boldsymbol{q}_{\mathrm{G}/0} + \tfrac{1}{2} \boldsymbol{q}_{\odot_1/\mathrm{I}} \boldsymbol{\omega}^{\odot_1}_{1/\odot_1} \boldsymbol{q}_{1/\odot_1} \boldsymbol{q}_{\mathrm{G}/1} \\
&\quad + \tfrac{1}{2} \boldsymbol{q}_{\odot_2/\mathrm{I}} \boldsymbol{\omega}^{\odot_2}_{2/\odot_2} \boldsymbol{q}_{2/\odot_2} \boldsymbol{q}_{\mathrm{G}/2} + \tfrac{1}{2} \boldsymbol{q}_{\odot_3/\mathrm{I}} \boldsymbol{q}_{\mathrm{e}/\odot_3} \boldsymbol{\omega}^{\mathrm{e}}_{\mathrm{e}/\odot_3} \boldsymbol{q}_{\mathrm{G/e}}.
\end{aligned} \tag{29}
$$

Finally, we simplify this expression to yield the kinematics of the end effector:

$$
\begin{aligned}
\dot{\boldsymbol{q}}_{\mathrm{G/I}} &= \tfrac{1}{2} \boldsymbol{q}_{\odot_0/\mathrm{I}} \boldsymbol{\omega}^{\odot_0}_{\odot_0/\mathrm{I}} \boldsymbol{q}_{\mathrm{G}/\odot_0} + \tfrac{1}{2} \boldsymbol{q}_{\odot_0/\mathrm{I}} \boldsymbol{\omega}^{\odot_0}_{0/\odot_0} \boldsymbol{q}_{\mathrm{G}/\odot_0} + \tfrac{1}{2} \boldsymbol{q}_{\odot_1/\mathrm{I}} \boldsymbol{\omega}^{\odot_1}_{1/\odot_1} \boldsymbol{q}_{\mathrm{G}/\odot_1} \\
&\quad + \tfrac{1}{2} \boldsymbol{q}_{\odot_2/\mathrm{I}} \boldsymbol{\omega}^{\odot_2}_{2/\odot_2} \boldsymbol{q}_{\mathrm{G}/\odot_2} + \tfrac{1}{2} \boldsymbol{q}_{\mathrm{e/I}} \boldsymbol{\omega}^{\mathrm{e}}_{\mathrm{e}/\odot_3} \boldsymbol{q}_{\mathrm{G/e}}.
\end{aligned} \tag{30}
$$

V. RESULTS

After discretizing the equations, we define the objective function to be minimized as $J(x_0, U) = (\boldsymbol{q}_{\mathrm{G/I}}(t_f) - \boldsymbol{q}_{\mathrm{D/I}})^{\mathrm{T}} W_{f,q} (\boldsymbol{q}_{\mathrm{G/I}}(t_f) - \boldsymbol{q}_{\mathrm{D/I}}) + \boldsymbol{\omega}^{\odot_0}_{\odot_0/\mathrm{I}}(t_f)^{\mathrm{T}} W_{f,\omega} \boldsymbol{\omega}^{\odot_0}_{\odot_0/\mathrm{I}}(t_f) + \sum_{k=0}^{N-1} (\boldsymbol{q}_{\mathrm{G/I}}(t_k) - \boldsymbol{q}_{\mathrm{D/I}})^{\mathrm{T}} W_{k,q} (\boldsymbol{q}_{\mathrm{G/I}}(t_k) - \boldsymbol{q}_{\mathrm{D/I}}) + \boldsymbol{\omega}^{\odot_0}_{\odot_0/\mathrm{I}}(t_k)^{\mathrm{T}} W_{k,\omega} \boldsymbol{\omega}^{\odot_0}_{\odot_0/\mathrm{I}}(t_k) + u(t_k)^{\mathrm{T}} R u(t_k)$. The penalty matrices were set to $W_{f,q} = 150 I_{8\times 8}$, $W_{f,\omega} = I_{8\times 8}$, $W_{k,q} = 15 I_{8\times 8}$, $W_{k,\omega} = I_{8\times 8}$ and $R = \mathrm{diag}(10 I_{3\times 3}, I_{3\times 3}, 0.01 I_{3\times 3}, 0.1 I_{3\times 3})$. Finally, the target pose for the end-effector, and the desired angular velocity of the base are given by $\boldsymbol{q}_{\mathrm{D/I}} = (0.5, [0.50, -0.50, -0.50]^{\mathrm{T}}) + \epsilon\,(0.25, [2.25, 0.25, 2.25]^{\mathrm{T}})$ and $\boldsymbol{\omega}^{\mathrm{D}}_{\mathrm{D/I}} = \mathbf{0}$ respectively.

The simulation was run for $T = 15\ s$, with $\Delta t = 0.015\ s$, and $N = 1,000$. The end-effector reference aims to achieve pose stabilization of the end-effector at a given desired pose, given that $\boldsymbol{q}_{\text{D/I}}$ is constant. Figure 2 shows snapshots from a time sequence of the trajectory after the convergence of the algorithm. The desired final frame is also shown in the figure and remains stationary throughout the maneuver. At the end of the maneuver, this frame is aligned with the local end-effector frame.

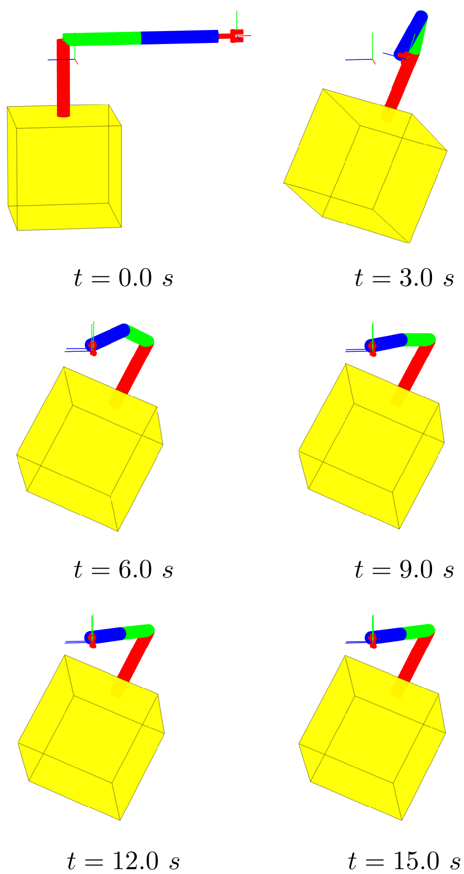

Fig. 2. Time sequence of end effector poses for stabilization maneuver.

The error pose of the end effector frame is computed via dual quaternions as

$$\boldsymbol{q}_{\text{D/G}} = \boldsymbol{q}^*_{\text{G/I}}\boldsymbol{q}_{\text{D/I}}. \tag{31}$$

The error quaternion and position vector error, expressed in the end-effector frame G, is shown in Figure 3 converging to their desired values. Figure 4 shows a scalar measure of both the angular and the linear errors. In the angular case, Figure 4 shows the Euler angle of the error rotation. The norm of the error vector is shown. Both of these quantities are directly derived from $\boldsymbol{q}_{\text{D/G}}$.

Figure 5 shows the actuation forces and torques applied on the base of the satellite. The cost function has been chosen so that the forces, usually generated by gas jet actuators contained on-board the spacecraft, are kept low since thruster firing requires fuel, which is a scarce resource in orbit. The torque generated is also low for this maneuver, but since it can be generated by reaction wheels, this component is penalized less aggressively in the cost term of the DDP formulation. Finally, Figure 6 shows the torques applied at each one of the three joints, and the Euler angle rates for the

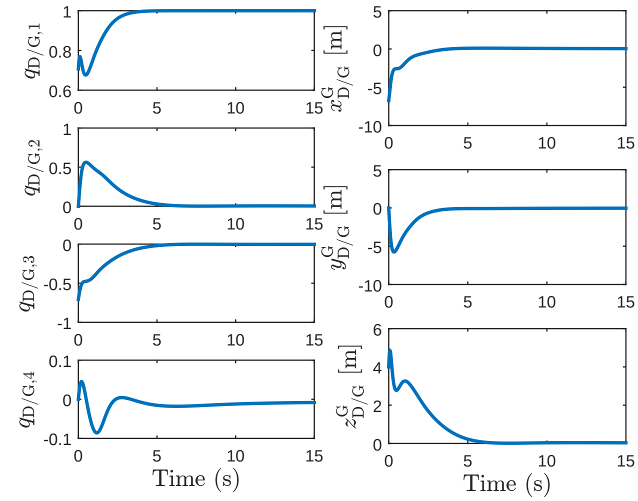

Fig. 3. Pose stabilization maneuver: quaternion error and position error.

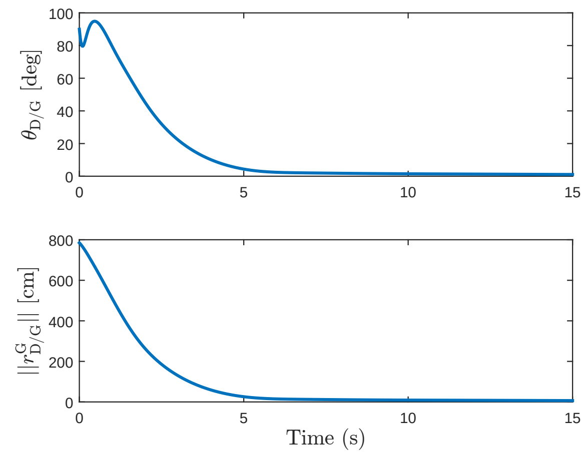

Fig. 4. Pose stabilization maneuver: error Euler angle and error vector norm.

end-effector motion (assumed for simplicity to represent the end-effector actuation mechanism). These are penalized less since they can be easily generated on-board the satellite.

VI. CONCLUSIONS

In this paper we have derived the dynamics of a robotic arm mounted on a free-floating satellite base using dual quaternion algebra. These dynamics were used in combination with DDP to perform a stabilization maneuver for the end effector. The framework provides for flexibility in the initial conditions of the system, not restricting the initial state of the system to having zero linear and angular momenta, and it seamlessly accounts for both thruster and momentum exchange actuation. The use of dual quaternions in the proposed framework enables the inclusion of tools typically used in fixed-base robotic systems, such as motions parameterized with screw-motion, which can be of much value during satellite servicing. Future work will focus on performing end-effector pose tracking, and on incorporating actuator dynamics to increase the fidelity of the simulator.

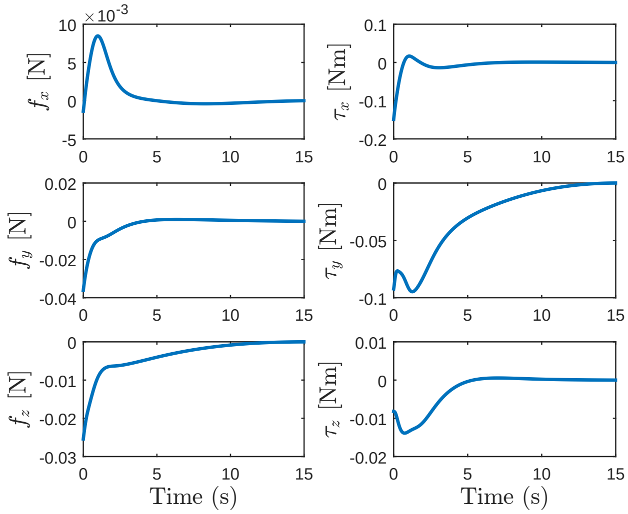

Fig. 5. Control effort: forces and torques applied at the satellite base.

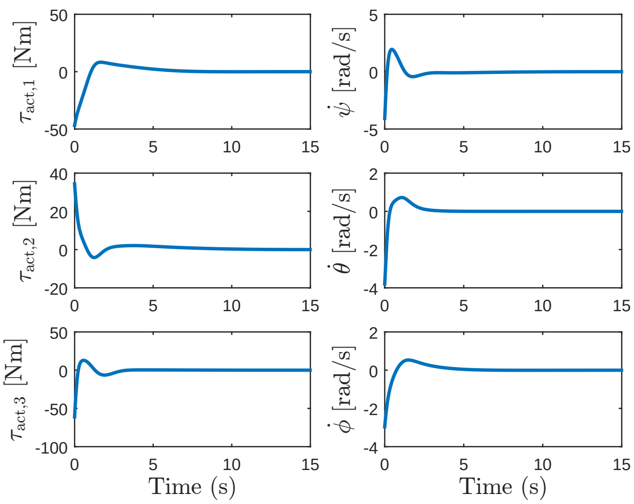

Fig. 6. Control effort: joint torques and Euler rates.

ACKNOWLEDGMENT

The authors would like to thank Dr. David S. Bayard at the G&C section at JPL for his valuable comments and guidance. This research was performed, in part, at the Jet Propulsion Laboratory, California Institute of Technology, under contract with the National Aeronautics and Space Administration, and funded through the internal Research and Technology Development program.

REFERENCES

[1] R. W. Longman, R. E. Lindbergt, and M. F. Zedd, "Satellite-mounted robot manipulators - new kinematics and reaction moment compensation," *The International Journal of Robotics Research*, vol. 6, no. 3, pp. 87–103, 1987.

[2] Z. Vafa and S. Dubowsky, "On the dynamics of manipulators in space using the virtual manipulator approach," in *Proceedings 1987 IEEE International Conference on Robotics and Automation*, March 31 - April 3 1987.

[3] Y. Masutani, F. Miyazaki, and S. Arimoto, "Modeling and sensory feedback control for space manipulators," in *Proceedings of the NASA Conference on Space Telerobotics*, no. 3, 1989, pp. 287 – 296.

[4] Z. Vafa and S. Dubowsky, "The kinematics and dynamics of space manipulators: The virtual manipulator approach," *The International Journal of Robotics Research*, vol. 9, no. 4, pp. 3–21, aug 1990.

[5] ——, "On the dynamics of space manipulators using the virtual manipulator, with applications to path planning," in *Space Robotics: Dynamics and Control*, X. Yangsheng and T. Kanade, Eds. Springer, 1993, pp. 45 – 76.

[6] Y. Umetani and K. Yoshida, "Resolved motion rate control of space manipulators with generalized jacobian matrix," *IEEE Transactions on Robotics and Automation*, vol. 5, no. 3, pp. 303–314, June 1989.

[7] A. Jain, "Unified formulation of dynamics for serial rigid multibody systems," *Journal of Guidance, Control, and Dynamics*, vol. 14, no. 3, pp. 531–542, May 1991.

[8] G. Rodriguez, A. Jain, and K. Kreutz-Delgado, "A spatial operator algebra for manipulator modeling and control," *The International Journal of Robotics Research*, vol. 10, no. 4, pp. 371–381, 1991.

[9] R. Featherstone and D. Orin, "Robot dynamics: equations and algorithms," in *Proceedings 2000 IEEE International Conference on Robotics and Automation*, vol. 1, 2000, pp. 826–834.

[10] J. R. Dooley and J. M. McCarthy, "On the geometric analysis of optimum trajectories for cooperating robots using dual quaternion coordinates," in *Proceedings 1993 IEEE International Conference on Robotics and Automation*, vol. 1, Atlanta, Georgia, May 2 – 6 1993, pp. 1031–1036.

[11] K. Daniilidis, "Hand-eye calibration using dual quaternions," *The International Journal of Robotics Research*, vol. 18, no. 3, pp. 286–298, March 1999.

[12] M. Ulrich and C. Steger, "Hand-eye calibration of SCARA robots using dual quaternions," *Pattern Recognition and Image Analysis*, vol. 26, no. 1, pp. 231–239, 2016.

[13] G. Leclercq, P. Lefèvre, and G. Blohm, "3-D kinematics using dual quaternions: Theory and applications in neuroscience," *Frontiers in Behavioral Neuroscience*, vol. 7, no. 7, pp. 1–7, February 2013.

[14] L. A. Radavelli, E. R. De Pieri, D. Martins, and R. Simoni, "Points, lines, screws and planes in dual quaternions kinematics," in *Advances in Robot Kinematics*, J. Lenarcic and O. Khatib, Eds. Springer, 2014, pp. 285–293.

[15] A. Perez, "Dual quaternion synthesis of constrained robotic systems," Ph.D. dissertation, Department of Mechanical and Aerospace Engineering, University of California, Irvine, September 2003.

[16] A. Perez and J. McCarthy, "Dual quaternion synthesis of constrained robotic systems," *Journal of Mechanical Design*, vol. 126, no. 3, pp. 425–435, September 2004.

[17] Y. Aydin and S. Kucuk, "Quaternion based inverse kinematics for industrial robot manipulators with Euler wrist," in *2006 IEEE International Conference on Mechatronics*, Budapest, Hungary, July 3 – 5 2006, pp. 581 – 586.

[18] J. Cheng, J. Kim, Z. Jiang, and W. Che, "Dual quaternion-based graphical SLAM," *Robotics and Autonomous Systems*, vol. 77, no. C, pp. 15–24, March 2016.

[19] N. Filipe and P. Tsiotras, "Adaptive position and attitude-tracking controller for satellite proximity operations using dual quaternions," *Journal of Guidance, Control, and Dynamics*, vol. 38, pp. 566–577, 2014.

[20] N. Filipe, M. Kontitsis, and P. Tsiotras, "Extended Kalman filter for spacecraft pose estimation using dual quaternions," *Journal of Guidance, Control, and Dynamics*, vol. 38, no. 9, pp. 1625 – 1641, September 2015.

[21] N. Filipe, "Nonlinear pose control and estimation for space proximity operations: An approach based on dual quaternions," Ph.D. dissertation, Georgia Institute of Technology, 2014.

[22] N. Filipe, A. Valverde, and P. Tsiotras, "Pose tracking without linear and angular-velocity feedback using dual quaternions," *IEEE Transactions on Aerospace and Electronic Systems*, vol. 52, no. 1, pp. 411–422, 2016.

[23] N. Filipe and P. Tsiotras, "Simultaneous position and attitude control without linear and angular velocity feedback using dual quaternions," in *Proceedings of the 2013 American Control Conference*, Washington, DC, June 17–19 2013, pp. 4815–4820.

[24] Y. Tassa, N. Mansard, and E. Todorov, "Control-limited differential dynamic programming," in *Proceedings 2014 IEEE International Conference on Robotics and Automation*, Hong Kong, China, May 31 – June 7 2014.